Numerical Analysis of a Weak Shock Wave Propagating in a Medium Using Lattice Boltzmann Method (LBM)

Ho-Keun Kang*
School of Mechanical and Aerospace Engineering · Institute of Marine Industry, Gyeongsang National University, 445 Inpyeong-dong, Tongyeong, Gyeongnam 650-160, Korea
Michihisa Tsutahara
Graduate School of Science and Technology, Kobe University, 1-1 Rokkodai, Nada, Kobe 657-8051, Japan
Ki-Deok Ro
School of Mechanical and Aerospace Engineering · Institute of Marine Industry, Gyeongsang National University, 445 Inpyeong-dong, Tongyeong, Gyeongnam 650-160, Korea
Young-Ho Lee
Division of Mechanical & Information Engineering, Korea Maritime University, 1 Dongsam-dong, Youngdo-ku, Busan 606-791, Korea

This study introduced a lattice Boltzmann computational scheme capable of modeling thermo hydrodynamic flows with simpler equilibrium particle distribution function compared with other models. The equilibrium particle distribution function is the local Maxwelian equilibrium function in this model, with all the constants uniquely determined. The characteristics of the proposed model is verified by calculation of the sound speeds, and the shock tube problem. In the lattice Boltzmann method, a thermal fluid or compressible fluid model simulates the reflection of a weak shock wave colliding with a sharp wedge having various angles θ_w. Theoretical results using LBM are satisfactory compared with the experimental result or the TVD.

Key Words : Computational Fluid Dynamics(CFD), Lattice Boltzmann Method(LBM), BGK Model, Compressible Fluid, Shock Wave, Reflection Wave

Nomenclature

c : Particle velocity
c_s : Sound speed
e : Internal energy
$f_{\sigma i}(t, \mathbf{r})$: Particle distribution function on $\mathbf{r}$ at t
P : Pressure
R : Radius of curvature
R^* : Gas constant
$\mathbf{r}$: Lattice node
T : Absolute temperature
t : Time
u_α : Fluid velocity

Greek symbols

γ : Coefficient of specific heats
ε : Knudsen number
χ : Thermal conductivity
λ : Second viscosity
μ : Viscosity
ρ : Density
σ : Number of speeds of particles
τ : Time increment
ϕ : Relaxation parameter
Ω : Collision operator

* Corresponding Author,
E-mail : kang88@gaechuk.gsnu.ac.kr
TEL : +82-55-640-3064; **FAX** : +82-55-640-3128
School of Mechanical and Aerospace Engineering · Institute of Marine Industry, Gyeongsang National University, 445 Inpyeong-dong, Tongyeong, Gyeongnam 650-160, Korea. (Manuscript **Received** September 13, 2002; **Revised** September 22, 2003)

Subscripts

α, β, γ : Cartesian coordinate

1. Introduction

Compared with the Navier-Stokes-based methods, the lattice Boltzmann method (LBM) (McNamara et al., 1988 ; Rothman et al., 1997 ; Wolf-Gladrow, 2000) has several advantages in simulating flows with highly complex geometries. Due to its cellular automata-based algorithm (Frisch et al., 1987) and its simple and efficient treatment of wall boundary conditions, simulations can be efficiently carried out on high performance vector-parallel computers with very high discretization on simple equidistant orthogonal lattices. Many theoretical and numerical studies tackling a variety of physics phenomena have been implemented, from shock formation to flows in porous media, magneto hydro-dynamics, phase separation, and turbulence.

A significant simplification of the original LBM was recently achieved by Chen et al.(1992, 1994) and Qian et al.(1992), applying the single relaxation time approximation of the Bhatnagar, Gross and Krook (BGK) method to the collision operator in the lattice Boltzmann equation. In this lattice BGK model, the local equilibrium particle distribution function is used to recover the Navier-Stokes equation.

In LBM, models for compressible or thermal fluids consider the conservation of kinetic energy of the particles in the collision stage. They require at least up to the third order term of fluid velocity in the equilibrium distribution functions.

Alexander et al.(1993) presented a two-speed model in the two-dimensional hexagonal lattice, wherein the equilibrium distribution function is expressed as the third order term of fluid velocity.

$$f_{\sigma i}^{(0)}=A_\sigma+B_\sigma \mathbf{c}_{\sigma i}\cdot\mathbf{u}+C_\sigma(\mathbf{c}_{\sigma i}\cdot\mathbf{u})^2+D_\sigma u^2 +E_\sigma(\mathbf{c}_{\sigma i}\cdot\mathbf{u})^3+F_\sigma(\mathbf{c}_{\sigma i}\cdot\mathbf{u})\,u^2 \quad (1)$$

where σ represents the number of speeds of the particles, in this case $\sigma=1, 2$, and the summation is not taken. However, the unknown parameters that are expressed by the density and the internal energy of the fluid become 14 ; thus, complicated calculations to determine them must be performed.

Chen et al.(1994) has presented a form that has a local equilibrium distribution function in the particle distribution model for one, two, and three-dimensional lattices up to the fourth term of the flow velocity.

$$f_{\rho ki}^{(0)}=A_{\rho k}+M_{\rho k}\mathbf{c}_{\rho ki}\cdot\mathbf{u}+G_{\rho k}u^2+J_{\rho k}(\mathbf{c}_{\rho ki}\cdot\mathbf{u})^2+Q_{\rho k}(\mathbf{c}_{\rho ki}\cdot\mathbf{u})\,u^2 +H_{\rho k}(\mathbf{c}_{\rho ki}\cdot\mathbf{u})^3+R_{\rho k}(\mathbf{c}_{\rho ki}\cdot\mathbf{u})^2u^2+S_{\rho k}u^4 \quad (2)$$

Here, the density and the internal energy also express the constants $A_{\rho k}$, $M_{\rho k}$, ···, $S_{\rho k}$ that determine the local equilibrium distribution function. The numbers are 32 for a two-dimensional case and 40 for a three-dimensional case. Like Alexander's model, they are not uniquely determined.

In this paper, the present work is different from the methods mentioned above, since it presents a simpler equilibrium distribution function compared with that of Alexander's or Chen's model. Likewise, the constants appearing in this function are uniquely determined. Using the simple model, the reflection phenomenon of a weak shock wave propagating in the shock tube with a wedge is simulated. The result is then compared with the TVD scheme and the experimental one.

2. Numerical Method

2.1 Lattice BGK model

The following lattice Boltzmann equation with BGK collision term describes the evolution of the distribution $f_{\sigma i}(t, \mathbf{r})$ at each lattice node $\mathbf{r}$, and time step t :

$$f_{\sigma i}(t+\tau, \mathbf{r}+\mathbf{c}_{\sigma i}\tau)-f_{\sigma i}(t, \mathbf{r})=\Omega_{\sigma i}, \quad (3)$$

where real number $f_{\sigma i}(t, \mathbf{r})$ is the mass of fluid at each lattice node $\mathbf{r}$, and time step t, moving in direction i with a speed of $|\mathbf{c}_{\sigma i}|=\sigma$, $\sigma=1, 2, \ldots, b$, where is the number of speed. The $\sigma=0$ speed corresponds to the component of the fluid at rest.

The microscopic dynamics associated with Eq. (3) can be viewed as a two-step process of movement and collision. During the movement step, $f_{\sigma i}(\mathbf{r}+\mathbf{c}_{\sigma i}\tau)$ is replaced by $f_{\sigma i}(\mathbf{r})$. Therefore, each site exchanges mass with its neighbors, i.e., sites

connected by lattice vectors $\mathbf{c}_{\sigma i}$. In the collision step, the distribution functions at each site relax toward a state of local equilibrium. For simplicity, the linear, singe time relaxation model of Bhatnagar, Gross, and Krook (BGK) that has been widely applied to LBM was used:

$$\Omega_{\sigma i}=-\frac{1}{\phi}[f_{\sigma i}(t,\mathbf{r})-f_{\sigma i}^{(0)}(t,\mathbf{r})]. \quad (4)$$

The collision operator $\Omega_{\sigma i}$ conserves the local mass, momentum and kinetic energy, while the parameter ϕ controls the rate at which the system relaxes to the local equilibrium of $f_{\sigma i}^{(0)}(t,\mathbf{r})$.

2.2 Local equilibrium distribution

The local Maxwellian equilibrium function f^{eq} for the kinetic theory is written as:

$$f^{eq}=\frac{\rho}{(2\pi R^*T)^{3/2}}\exp\left[-\frac{(c_\alpha-u_\alpha)^2}{2R^*T}\right](\alpha=x,\ y,\ z) \quad (5)$$

where R^* is the gas constant, T the absolute temperature, u_α and c_α the fluid velocity and the molecular velocity, respectively. Subscript α represents the Cartesian coordinates.

The equilibrium function can be obtained at a small Mach number of the flow through truncation of the Taylor expansion of f^{eq} up to third-order in $\mathbf{u}$:

$$f^{eq}=Ae^{Bc^2}\rho[1-2Bc_\alpha u_\alpha+2B^2c_\alpha c_\beta u_\alpha u_\beta +BU^2-2Bc_\alpha u_\alpha u^2-\frac{4}{3}B^3c_\alpha c_\beta c_\gamma u_\alpha u_\beta u_\gamma] \quad (6)$$

where

$$A=\frac{1}{(2\pi R^*T)^{3/2}},\quad B=-\frac{1}{(2R^*T)}. \quad (7),(8)$$

The particle velocities are then discretized. These constants are determined from the constraints so that the Navier-Stokes equations are derived from the distribution function in Eq. (3).

The hexagonal lattice (FHP lattice) is considered in 2-D calculation together with unit spacing, wherein each node has six nearest neighbors connected by six links. Particles can only reside on the nodes and move to their nearest neighbors along the links in unit time. There are 13 particles consisting of two-speed particles c and $2c$, including the rest particle. Thus, the equilibrium distribution function is written as

$$f_{\sigma i}^{eq}=A_ie^{Bc^2\sigma}\rho[1-2Bc_{\sigma i\alpha}u_\alpha+2B^2c_{\sigma i\alpha}c_{\sigma i\beta}u_\alpha u_\beta+Bu^2 -2Bc_{\sigma i\alpha}u_\alpha u^2-\frac{4}{3}B^3c_{\sigma i\alpha}c_{\sigma i\beta}c_{\sigma i\gamma}u_\alpha u_\beta u_\gamma] \quad (9)$$

where σ=I and II correspond the particle speed c and $2c$, respectively. Likewise, i=0 corresponds the rest particle.

$$\begin{aligned}&\text{for}\quad i=0,\quad e^{Bc^2\sigma}=1\ (\because c_\sigma=0)\\ &\text{for}\quad i\neq0,\quad e^{Bc^2\sigma}=e^{Bc^2\mathrm{I}}=e^{Bc^2}\quad(\sigma=1)\\ &\qquad e^{Bc^2\sigma}=e^{Bc_{\mathrm{II}}^2}=e^{B4c^2}(\sigma=\mathrm{II},\ c_{\mathrm{II}}=2c_{\mathrm{I}})\end{aligned} \quad (10)$$

The coefficient $A_ie^{Bc^2\sigma}=F_{\sigma i}$ varies from particle to particle, Eq. (9) is therefore written as:

$$f_{\sigma i}^{eq}=F_\sigma\sigma[1-2Bc_{\sigma i\alpha}u_\alpha+2B^2c_{\sigma i\alpha}c_{\sigma i\beta}u_\alpha u_\beta+Bu^2 -2Bc_{\sigma i\alpha}u_\alpha u^2-\frac{4}{3}B^3c_{\sigma i\alpha}c_{\sigma i\beta}c_{\sigma i\gamma}u_\alpha u_\beta u_\gamma] \quad (11)$$
$$(\sigma=\mathrm{I},\ \mathrm{II},0\ \ i=0,\ 1,\ ...,\ 6)$$

where $F_{\mathrm{II}}=F_{\mathrm{I}}$, $F_{\mathrm{III}}=F_{\mathrm{II}}$ is written since particle numbers in all directions are the same at zero fluid velocity. The constants being determined are B, F_0, F_{I}, F_{II}. Actually, the expansion of u in the equilibrium distribution function up to the second order sufficiently determines the above mentioned 4 constants. The third order term is necessary for the energy conservation equation.

The equilibrium distribution function $f_{\sigma i}^{(0)}$ up to the second order is written as:

$$f_{\sigma i}^{(0)}=F_\sigma\rho[1-2Bc_{\sigma i\alpha}u_\alpha+2B^2c_{\sigma i\alpha}c_{\sigma i\beta}u_\alpha u_\beta+Bu^2]. \quad (12)$$

The coefficients F_σ, B are functions of density ρ, internal energy e, and mass, momentum, and internal energy at the collision of the particles is also conserved. Then, the relations between the distribution functions and the variables of macroscopic fluid are:

$$\text{Density}: \sum_{\sigma,i}f_{\sigma i}=\sum_{\sigma,i}f_{\sigma i}^{(0)}=\rho \quad (13)$$

$$\text{Momentum}: \sum_{\sigma,i}f_{\sigma i}c_{\sigma i\alpha}=\sum_{\sigma,i}f_{\sigma i}^{(0)}c_{\sigma i\alpha}=\rho u_\alpha \quad (14)$$

$$\text{Energy}: \sum_{\sigma,i}\frac{1}{2}f_{\sigma i}c_\sigma^2=\sum_{\sigma,i}\frac{1}{2}f_{\sigma i}^{(0)}c_\sigma^2=\frac{1}{2}\rho u^2+\rho e. \quad (15)$$

Using the constraints on the isotropic property of the tensor, the parameters of the equilibrium distribution function is determined as:

$$\begin{cases} F_0=1-\dfrac{1}{4B^2c^4}(2+5Bc^2) \\ F_{\mathrm{I}}=-\dfrac{1}{9B^2c^4}(1+2Bc^2),\ F_{\mathrm{II}}=\dfrac{1}{36B^4c^4}(1+\dfrac{1}{2}Bc^2) \quad (16)\sim(19) \\ B=-\dfrac{1}{2e} \end{cases}$$

2.3 Governing equations

To recover the desired thermal Navier-Stokes equations, the discrete lattice Boltzmann equation into the continuous space and time form by Tayor expanding Eq. (3) on ($\mathbf{r}$, t) up to the second order of flow velocity is translated as:

$$\partial_t f_{\sigma i}+c_{\sigma i\alpha}\partial_\alpha f_{\sigma i}+\frac{1}{2}\tau c_{\sigma i\alpha}c_{\sigma i\beta}\partial_\alpha\partial_\beta f_{\sigma i}+\tau c_{\sigma i\alpha}\partial_t\partial_\alpha f_{\sigma i} +\frac{1}{2}\tau\partial_t^2 f_{\sigma i}=-\frac{1}{\tau\phi}(f_{\sigma i}-f_{\sigma i}^{(0)}) \tag{20}$$

The subindices α and β represent Cartesian components with summation over repeated subscripts. The Chapmann-Enskog procedure is therefore employed, assuming the following multi-scale expansion for the time and spatial derivatives in a small quantity ε:

$$\partial_t \to \varepsilon\partial_{t1}+\varepsilon^2\partial_{t2},\ \partial_\alpha \to \varepsilon\partial_\alpha \tag{21}$$

where ε is the Knudsen number. The distribution function is also expanded as:

$$f_{\sigma i}=f_{\sigma i}^{(0)}+f_{\sigma i}^{neq}=f_{\sigma i}^{(0)}+\varepsilon f_{\sigma i}^{(1)}+\varepsilon^2 f_{\sigma i}^{(2)}+\cdots. \tag{22}$$

Substituting of Eq. (21) and Eq. (22) with Eq. (20), and taking the terms up to the second order of ε produces the following equation:

$$(\partial_{t1}+\partial_{t2})f_{\sigma i}^{(0)}+c_{\sigma i\alpha}\partial_\alpha f_{\sigma i}^{(0)}+\left(1-\frac{1}{2\phi}\right) [\partial_t f_{\sigma i}^{(1)}+c_{\sigma i\alpha}\partial_\alpha f_{\sigma i}^{(1)}]=-\frac{1}{\tau\phi}(f_{\sigma i}^{(1)}+f_{\sigma i}^{(2)}). \tag{23}$$

Hereafter, this paper used $\partial_{t1}+_{t2}=\partial_t$.

2.3.1 Equation of continuity

Summing up the terms in Eq. (23) with respect to produces the following equation:

$$(\partial_t+c_{\sigma i\alpha}\partial_\alpha)\sum_{\sigma,i}f_{\sigma i}^{(0)}=0. \tag{24}$$

Substituting Eq. (13) and Eq. (14) with Eq. (24), the alternate equation of continuity is written as:

$$\partial_t\rho+\partial_\alpha(\rho u_\alpha)=0. \tag{25}$$

2.3.2 Equations of motion

Multiplying Eq. (23) by particle velocity $c_{\sigma i\alpha}$ and summing up σ and i, the equation is changed as:

$$(\partial_t+c_{\sigma i\beta}\partial_\beta)\sum_{\sigma,i}f_{\sigma i}^{(0)}c_{\sigma i\alpha}-\tau\left(\phi-\frac{1}{2}\right)\partial_\beta [(\partial_t+c_{\sigma i\gamma}\partial_\gamma)\sum_{\sigma,i}f_{\sigma i}^{(0)}c_{\sigma i\alpha}c_{\sigma i\beta}]=0 \tag{26}$$

Considering Eq. (23) and the isotropy of the tensors produces the following equation:

$$\partial_t(\rho u_\alpha)+\partial_\beta(\rho u_\alpha u_\beta)=-\partial_\alpha P+\partial_\beta [\mu(\partial_\alpha u_\beta+\partial_\beta u_\alpha)]+\partial_\alpha(\lambda\partial_\gamma u_\gamma) \tag{27}$$

In identifying the transport coefficients in Eq. (27) with the corresponding terms in the thermal Navier-Stokes equations, the values of pressure P, viscosity μ and second viscosity λ are determined as

$$P=\frac{2}{D}\rho e,\ \mu=\frac{2}{D}\rho e\tau\left(\phi-\frac{1}{2}\right),\ \text{and}\ \lambda=-\frac{4}{D^2}\rho e\tau\left(\phi-\frac{1}{2}\right)=-\mu,$$

respectively. (28) ~ (30)

2.3.3 Equation of energy

Multiplying (23) by $c_\sigma^2/2$, summing up σ and i, and considering the conditions for the non-equilibrium part of the distribution functions produces the following equation:

$$(\partial_t+c_{\sigma i\alpha}\partial_\alpha)\sum_{\sigma,i}\frac{1}{2}f_{\sigma i}^{(0)}c_\alpha^2-\tau\left(\phi-\frac{1}{2}\right)\partial_\alpha \left[(\partial_t+c_{\sigma i\beta}\partial_\beta)\sum_{\sigma,i}\frac{1}{2}f_{\sigma i}^{(0)}c_{\sigma i\alpha}c_\sigma^2\right]=0 \tag{31}$$

The first term in Eq. (31) is derived from Eq. (15) and is written as:

$$\partial_t\sum_{\sigma,i}\frac{1}{2}f_{\sigma i}^{(0)}c_\sigma^2=\partial_t\left(\rho e+\frac{1}{2}\rho u^2\right) \tag{32}$$

The second term in Eq. (31) must correspond to the following equation:

$$\frac{1}{2}c_{\sigma i\alpha}c_\sigma^2\partial_\alpha f_{\sigma i}^{(0)}=u_\alpha\partial_\alpha\left(\rho e+P+\frac{1}{2}\rho u^2\right) \tag{33}$$

Based on the above term, the equilibrium distribution function $f_{\sigma i}^{(0)}$ in Eq. (11) must contain the third term of $\mathbf{u}$ written as:

$$f_{\sigma i}^{eq}=F_\sigma\rho[1-2Bc_{\sigma i\alpha}u_\alpha+2B^2c_{\sigma i\alpha}c_{\sigma i\beta}u_\alpha u_\beta+Bu^2+mc_{\sigma i\alpha}u_\alpha u^2+nB^3c_{\sigma i\alpha}c_{\sigma i\beta}c_{\sigma i\gamma}u_\alpha u_\beta u_\gamma] \tag{34}$$

Determining the parameters m, n to satisfy Eqs.

(15) and (33) produces the following equation:

$$m=-\frac{F_{\mathrm{I}}+16F_{\mathrm{II}}}{108c^4F_{\mathrm{I}}F_{\mathrm{II}}} \text{ and } n=\frac{F_{\mathrm{I}}+4F_{\mathrm{II}}}{81c^6F_{\mathrm{I}}F_{\mathrm{II}}}. \quad (35),(36)$$

Substituting $f_{\sigma i}^{(0)}$ with Eq. (31), the equation of energy is derived as:

$$\partial_t\left(\rho e+\frac{1}{2}\rho u^2\right)+\partial_\alpha\left(\rho e+P+\frac{1}{2}\rho u^2\right)u_\alpha=\partial_\alpha(\chi\partial_\alpha e) +\partial_\alpha\left[\rho\chi\tau\left(\phi-\frac{1}{2}\right)(\partial_\alpha u_\beta+\partial_\beta u_\alpha)u_\beta+\left(1-\frac{e}{\chi}\right)\partial_\gamma u_\gamma\delta_{\alpha\beta}\right] \quad (37)$$

The thermal conductivity χ is written as:

$$\chi=2\rho e\tau\left(\phi-\frac{1}{2}\right) \quad (38)$$

The macroscopic equations are derived and the equilibrium distribution function for this lattice BGK model $f_{\sigma i}^{(0)}$ is determined.

Many gases can be represented accurately by the following ideal gas equation:

$$P=(\gamma-1)\rho e \quad (39)$$

where γ is the adiabatic index of the gas. Comparing Eq. (28) with Eq. (39) reveals that following the above formulations would produce the following coefficient of specific γ value:

$$\gamma=\frac{D+2}{D} \quad (40)$$

Therefore the sound speed c_s in the two-dimensional model presented is written as:

$$c_s=\sqrt{\gamma\frac{P}{\rho}}=\sqrt{\frac{D+2}{D}\frac{\rho e}{\rho}}=\sqrt{2e} \quad (41)$$

3. Numerical Simulation

3.1 Shock tube problems

The sound speed is expressed by Eq. (41) as a function of the internal energy, and this expression is confirmed for various values of the internal energy. The flow employed is considered a shock tube, in which the two regions are separated initially at the center of the square duct. The number of the lattice is 400×20. The left region is occupied by higher-pressure gas and the right region by lower-pressure gas, and the separation is removed suddenly. When the pressure difference is very small, sound waves propagate from the center towards both directions. On the other hands, when the pressure difference is large, a shock wave runs rightward and the rarefaction waves propagate leftward. The boundary conditions on the top and bottom walls are periodic and those on the right and the left walls are slip and bounce-back, and therefore thermally adiabatic conditions. The sound speeds c_s obtained by changing the initial condition are shown in Table 1 and compared with the theoretical values in Eq. (41).

Table 1 Comparison between theoretical and calculated values of sound speed

e_4	e_1	ρ_4	ρ_1	c_s (LBM)	c_s (theory)
0.26	0.26	12.1	12.0	0.72	0.721
0.30	0.30	12.1	12.0	0.77	0.775
0.32	0.32	12.1	12.0	0.79	0.80
0.40	0.40	12.1	12.0	0.89	0.894
0.50	0.50	12.1	12.0	0.99	1.0
0.263	0.26	12.0	12.0	0.72	0.721
0.303	0.30	12.0	12.0	0.77	0.775
0.404	0.40	12.0	12.0	0.88	0.894
0.505	0.50	12.0	12.0	0.98	1.0

The distances of the point where the slope of the pressure has maximum value from the center at two different times are detected, and the propagation speed is determined. The calculated sound speeds are very compatible with the theoretical ones.

The shock tube problem is described above and the pressure relationship is expressed as

$$\frac{p_4}{p_1}=\frac{p_2}{p_1}\left[1-\frac{(\gamma_4-1)(e_1/e_4)(p_2/p_1-1)}{\sqrt{2\gamma_1}\sqrt{2\gamma_1(\gamma_1+1)(p_2/p_1-1)}}\right]^{-\frac{2\gamma_4}{(\gamma_4-1)}} \quad (42)$$

where p_2 is the pressure just behind the shock. The shock Mach number $M_s=U_s/c_{s1}$ is also related to the pressure ratio as

$$\frac{p_4}{p_1}=\frac{2\gamma_1M_s^2-(\gamma_1-1)}{\gamma_1+1}\left[1-\frac{\gamma_4-1}{\gamma_1-1}\frac{e_1}{e_4}\left(M_s-\frac{1}{M_s}\right)\right]^{-\frac{2\gamma_4}{\gamma_4-1}} \quad (43)$$

In above equation $\gamma_1=\gamma_4=2$, then the comparisons are presented in Table 2 between the calculated value and the theoretical ones for various p_4/p_1 and e_1/e_4. The figures shown in this table shows that if the difference between the

Table 2 Comparison between theoretical and calculated values of shock Mach number and pressure ratio

p_4/p_1	e_4/e_1	p_2/p_1 (LBM)	p_2/p_1 (theory)	M_s (LBM)	M_s (theory)
4.0	1.0	1.88	1.885	1.28	1.290
3.0	1.0	1.66	1.669	1.21	1.225
2.0	1.0	1.39	1.393	1.11	1.138
3.0	1.5	1.77	1.864	1.27	1.284
2.5	1.5	1.62	1.690	1.21	1.232
1.5	1.5	1.25	1.269	1.08	1.096
3.0	2.0	1.84	2.010	1.28	1.326
2.0	2.0	1.47	1.566	1.16	1.194

internal energies at the initial stage becomes larger the error may not be negligible but that if the differences si small the error can be negligibly small.

3.2 Shock reflection

Consider a planar incident shock wave at the initial state with a Mach number M_s colliding with a sharp wedge having an angle θ_w (Fig. 1). A shock reflection phenomenon on the wedge is the fundamental problems of compressible flows. This type of reflection is simulated in the proposed model with the simplified equilibrium distribution function. The number of the lattice is 1680×1040 and the corner of the wedge is located at (450, 0), with the origin at the left corner. The half angle of the wedge θ_w is from 5 to 25 degree, with the diaphragm located at $x=250$. The density in the lower pressure chamber is $\rho_1=12.0$ and $\rho_4=25.41$ in the high-pressure chamber. The internal energies at the initial stage are $e_1=e_4=0.4$. The boundary on the inclined plane has a non-slip condition considering the equilibrium distribution function, with those on the other walls having mirrored reflection slip conditions. For the temperature of the internal energy, adiabatic condition is applied.

Figure 2 shows the result for the half angle of 15 degree, wherein this weak shock displays is a Von Neumann reflection (Gabi, 1992). These results are consistent with the experimental results (Sasoh et al., 1992) shown in Fig. 3.

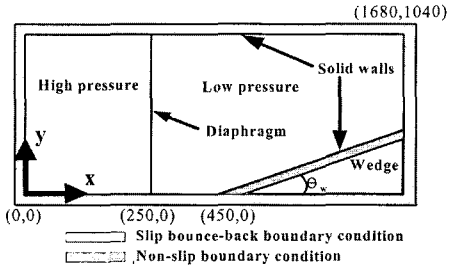

Fig. 1 Simulated flow field over a wedge with angle θ_w

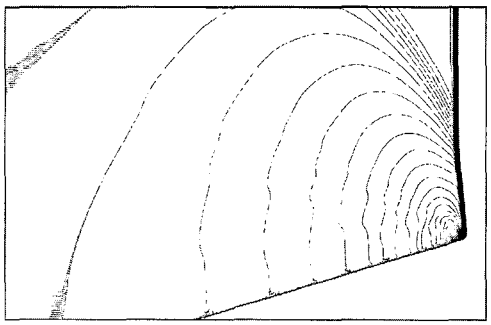

Fig. 2 Reflection of a shock wave over a wedge (Angle of wedge : 15 degree, $M_s=1.15$)

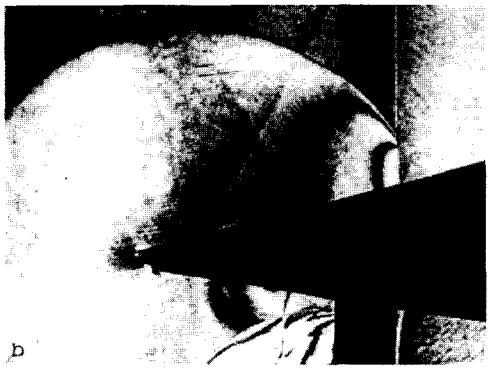

Fig. 3 Schilieren photograph of a shock wave over a wedge (Sasoh et al., 1992)

The radius of curvature of the incident shock surface is compared with previously reported results : TVD simulation and the experiments for the same half angle (Sasoh et al., 1992). The position of the shock surface is identified by the y axis measured perpendicular to the wedge surface. The result presented in Fig. 5 shows a non-dimensional radius of curvature and position by the distance L_s of the incident shock from the wedge front shown in Fig. 4.

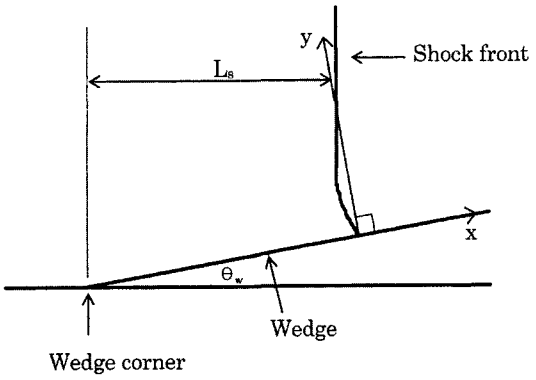

Fig. 4 Definition sketch of the shock and wedge position

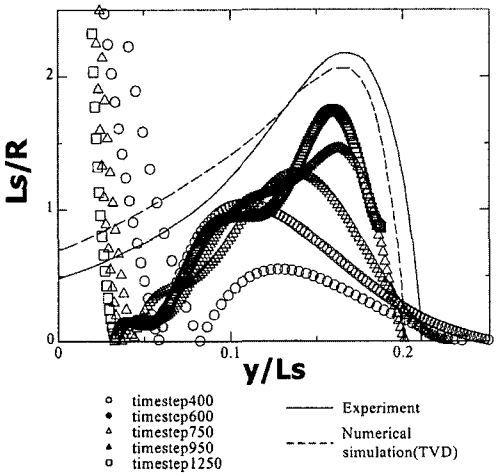

Fig. 5 Non-dimensional radius of curvature

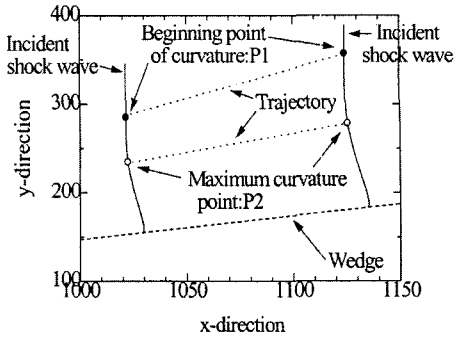

Fig. 6 Trajectory of an incident shock wave

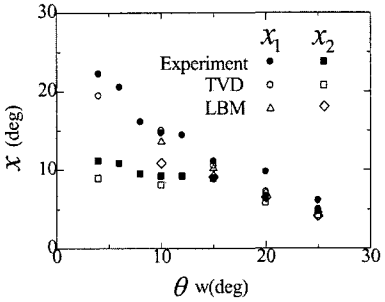

Fig. 7 Angles x_1 and x_2 between the x-axis line and trajectories of points P_1 and P_2. Experimental and TVD results are shown by Sasoh et al. (1992)

The result shows that the maximum of the radius of curvature R grows larger in time. However, the radius obtained by the present method is still a little smaller than the experimental result or the TVD simulation. The difference from the TVD simulation is due to the Reynolds number difference; in the present calculation, the Reynolds number is 1.2×10^4. In contrast, the Euler equation is solved in the TVD simulation.

It is particularly noted in the calculation that the curvature y/L_s in the vicinity of the wedge surface is inverted and smaller than 0.1. It also approaches zero L_s/R as it goes faster, which is a drawback of the reset calculation. This phenomenon is considered to be due to the Knudsen layer (Cornubert et al., 1991), which is a layer wherein the state of the distribution function is far away from the equilibrium (Tsutahara et al., 2002) near the solid surface. The state then becomes non-equilibrium, with the fluid behavior different from that obtained by the Navier-Stokes equations. This point should be studied more precisely in the future.

Further comparison was made for the shock wave shape. First, a point indicated as P_1 was detected wherein the shock starts to curve. Another point indicated as P_2 was also noted wherein the curvature reached its maximum (the radius of curvature is minimum). The trajectories of both points were obtained. These trajectories turned out to be straight line (Fig. 6), with the angles between those lines and the edge surface expressed by χ_1 and χ_2, respectively, to correspond to P_1 and P_2. Figure 7 shows the relationship between χ_1, χ_2 and the angle of the wedge θ_w and how they are in agreement with each other, especially when

the wedge angle is large.

4. Conclusion

A simplified model with an equilibrium distribution function is proposed for the thermal lattice BGK equation and this model is shown to simulate compressible flows successfully.

The two-dimensional weak shock reflection at the wedge for various θ_w are simulated. The result shows that the maximum radius obtained by the proposed method is still a little smaller compared with the experimental result or the TVD scheme, due to the Reynolds number difference.

The comparison of the radius of curvature at various angles indicates that LBM is compatible with the experimental result or the TVD scheme.

Acknowledgement

This work was supported by the Brain Korea 21 Project.

References

Alexander, F. J., Chen, S. and Sterling, D. J., 1993, "Lattice Boltzmann thermodynamics," Physical Review E, Vol. 47, pp. 2249~2252.

Chen, H., Chen, S. and Matthaeus, W. H., 1992, "Recovery of the Navier-Stokes Equations Using a Lattice-Gas Boltzmann Method," Physical Review A, Vol. 45, pp. R5339~5342.

Chen, Y., Ohashi, H. and Akiyama, M., 1994, "Thermal Lattice Bhatnagar Gross Krook Model without Nonlinear Deviations in Macrodynamic Equations," Physical Review E, Vol. 50, pp. 2776~2783.

Cornubert, R., d'Humiere, D. and Levermoer, D., 1991, "A Knudsen layer theory for lattice gases," Physica D, Vol. 47, pp. 241~259.

Frisch, U., Hasslacher, B. and Pomeau, Y., 1986, "Lattice-Gas Automata for the Navier-Stokes Equation," Physical Review Letters, Vol. 55, pp. 1505~1508.

Gabic, B. D., 1992, "Shock Wave Reflection Phenomena," Springer Verlag.

McNamara, G. and Zannetti, G., 1988, "Use of the Boltzmann Equation to Simulate Lattice Gas Automata," Physical Review Letters, Vol. 61, pp. 2332~2335.

Qain, Y. H., D'Humieres, D. and Lallemand, P., 1992, "Lattice BGK models for Navier-Stokes Equation," Europhysis Letters, Vol. 17, pp. 479~484.

Rothman, D. H. and Zaleski, S., 1997, "Lattice-Gas Celluar Automata-Simple Models of Complex Hydrodynamics," Cambridge University Press.

Sasoh, A., Takayama, K. and Saito, T., 1992, "A weak shock wave reflection over wedge," Shock Waves 2, pp. 277~281.

Tsutahara, M. and Kang, H. K., 2002, "A Discrete Effect of the Thermal Lattice BGK Model," Journal of Statistical Physics, Vol. 107, No. 112, pp. 479~498. c_s

Wolf-Gladrow, D. A., 2000, "Lattice-gas Cellular Automata and Lattice Boltzmann Models," Lecture Notes in Mathematics, Springer. M_s